ONE-THIRD SCALE MODEL OF AN OFFSET FED SCANNING ANTENNA FOR THE SHUTTLE IMAGING MICROWAVE SYSTEM

Report No. TR072
Final Report
JPL Contract No. 954145

Prepared for:

JET PROPULSION LABORATORY
California Institute of Technology
4800 Oak Grove Drive
Pasadena, California 91103

Prepared by:

J.H. Gustincic
Consulting Engineer
13121 Mindanao Way
Marina Del Rey, California 90291

25 November 1975

This work was performed for the Jet Propulsion Laboratory, California Institute of Technology, sponsored by the National Aeronautics and Space Administration under Contract NAS7-100

(NASA-CR-146081) ONE-THIRD SCALE MODEL OF AN OFFSET FED SCANNING ANTENNA FOR THE SHUTTLE IMAGING MICROWAVE SYSTEM Final Report (Gustincic (J. H.) Cousulting Engineer) 31 p HC $4.00 CSCL 17I G3/32

N76-15332

Unclas
07449

This report contains information prepared by J.J. Gustincic under JPL subcontract. Its content is not necessarily endorsed by the Jet Propulsion Laboratory, California Institute of Technology, or the National Aeronautics and Space Administration.

ABSTRACT

This report describes the results of an experimental study involving the design, fabrication and measurement of a one-third scale model of the 4m diameter parabolic torus reflector with a Gregorian feed for the SIMS application. Antenna pattern measurements of the model at 60 and 30 Ghz are presented to verify the predictions of a geometrical optics analysis upon which the antenna design was based. It is shown that the antenna measurements bear out the geometrical optics analysis in every respect and that the Gregorian subreflector feed is useable at all frequencies above at least 10 Ghz in the full size SIMS antenna. The fabricat' n of the model antenna is discussed in detail including a computerized technique for fabricating the transcendental subreflector shape with a numerically controlled machine.

TABLE OF CONTENTS

1.0 INTRODUCTION

This report describes the results of a three-man month study undertaken to verify the high frequency performance of a 4m parabolic torus antenna system for the Shuttle Imaging Microwave System (SIMS). This antenna system is designed for simultaneous operation at eleven frequencies between .610 and 118.7 Ghz utilizing point source feeds at the lower frequencies and Gregorian subreflector feed systems at the higher frequencies. The low performance of the parabolic torus has been verified by experimental measurements on a one-tenth scale model at about 6 Ghz. The results of these measurements and a detailed description of the entire antenna system is included in a previous interim report(1) as well as the results of a theoretical geometrical optics calculation predicting good antenna performance at the higher frequencies. It is the purpose of the portion of the study described in this report to construct and measure a one-third scale model for use at 60 and 30 Ghz in order to verify the high frequency performance characteristics of the full size Torus-Gregorian combination at 20 and 10 Ghz.

The one-third scale model is shown in Fig. 1 along with the one-tenth scale model previously mentioned. Since an evaluation of only the electrical antenna performance was the objective of this study the one-third scale model was constructed without the rotating feed support wheel. As seen in the figure, a single subreflector with a horizontally polarized feed horn is supported on two fixed rails in the position it would have if it were on the wheel illuminating the central portion of the torus. The full model assembly as shown is approximately 54" wide, 26" high and weighs about 160 lbs. The reflector is believed to have an rms surface tolerance of a

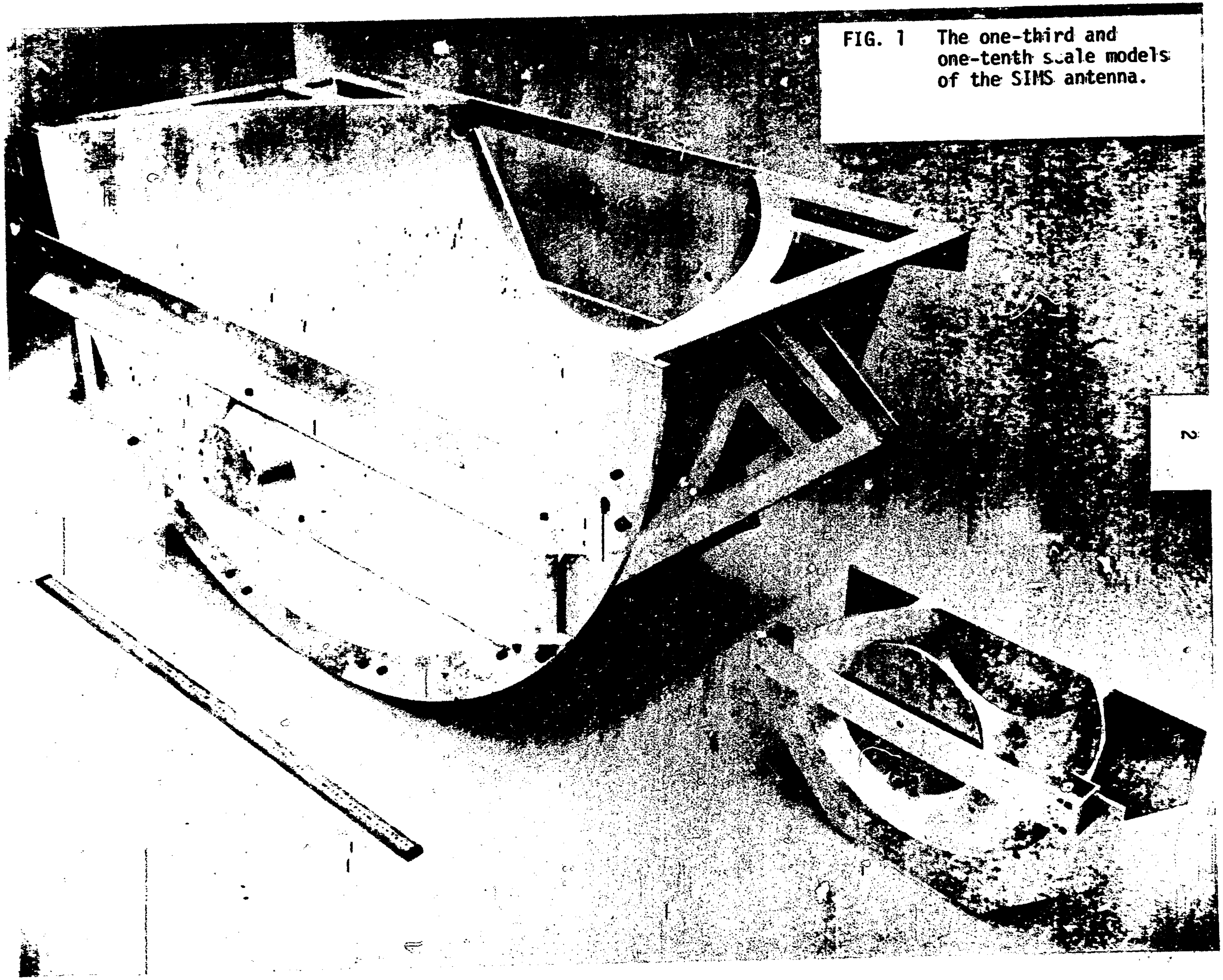

FIG. 1 The one-third and one-tenth scale models of the SIMS antenna.

ORIGINAL PAGE IS
OF POOR QUALITY

few mills. The interchangeable feed horns were provided for use in illuminating the subreflector at the respective frequencies of 30 and 60 Ghz. Section 2 of this report deals with a summary of the measurements made on the one-third scale model while Section 3 deals with the design and fabrication of the model.

2.0 SUMMARY OF THE EXPERIMENTAL RESULTS

2.1 60 Ghz Measurements

The main experimental emphasis was placed on measurements at 60 Ghz in order to obtain a verification of the geometrical optics calculations which predicted successful antenna performance at the higher frequencies. The performance of the one-third scale model was measured on the 1200 foot Mesa antenna range at JPL. The measured 60 Ghz antenna patterns for the principal and diagonal places for the principal and cross polarizations are shown in Figs. 2, 3 and 4. The beam shapes, sidelobe levels and beamwidths are in excellent agreement with the geometrical optics predictions of the interim report.(1) As can be seen in the Figures, the cross polarized beams due to the reflector curvature and offset feed arrangement are in the diagonal plane and are about 18 db down from the peak of the main beam.

The antenna patterns were integrated and the comparison between the measured values and the results of the geometrical optics analysis are presented in Table I. As can be seen, the measured and computed beamwidths are almost identical. In a manner consistent with the work of the interim report,(1) the beam efficiency in Table I is defined as the fraction of the principally polarized energy contained within a full width of 1.576° around boresight. This angle corresponds to the narrowest width of the main beam which occurs in the diagonal plane. As shown in the table, the measured beam efficiency is a few percent higher than the computed values. The biggest discrepancy occurs in the fraction of the total power which appears in cross polarization. The geometrical optics analysis gives a value of 1.8% as compared with the measured value of 4% which is still quite acceptable for the SIMS application. This discrepancy probably occurs due to the

TABLE I

Comparison of Experimental Results and Geometrical Optics Calculations

	One-third scale model measurements at 60 Ghz	Full size antenna performance at 20 Ghz as computed from geometrical optics
Feed Type:	Horizontally polarized rectangular horn	Assumed Gaussian beam shape
Track plane 3 db: beamwidth	.667°	.669°
Scan plane 3 db: beamwidth	.611°	.615°
Diagonal plane 3 db: beamwidth	.611°	.631°
Beam efficiency: (Excluding Cross Polarization)	93.4%	91%
Fraction of total: power in cross polarization	4%	1.8%

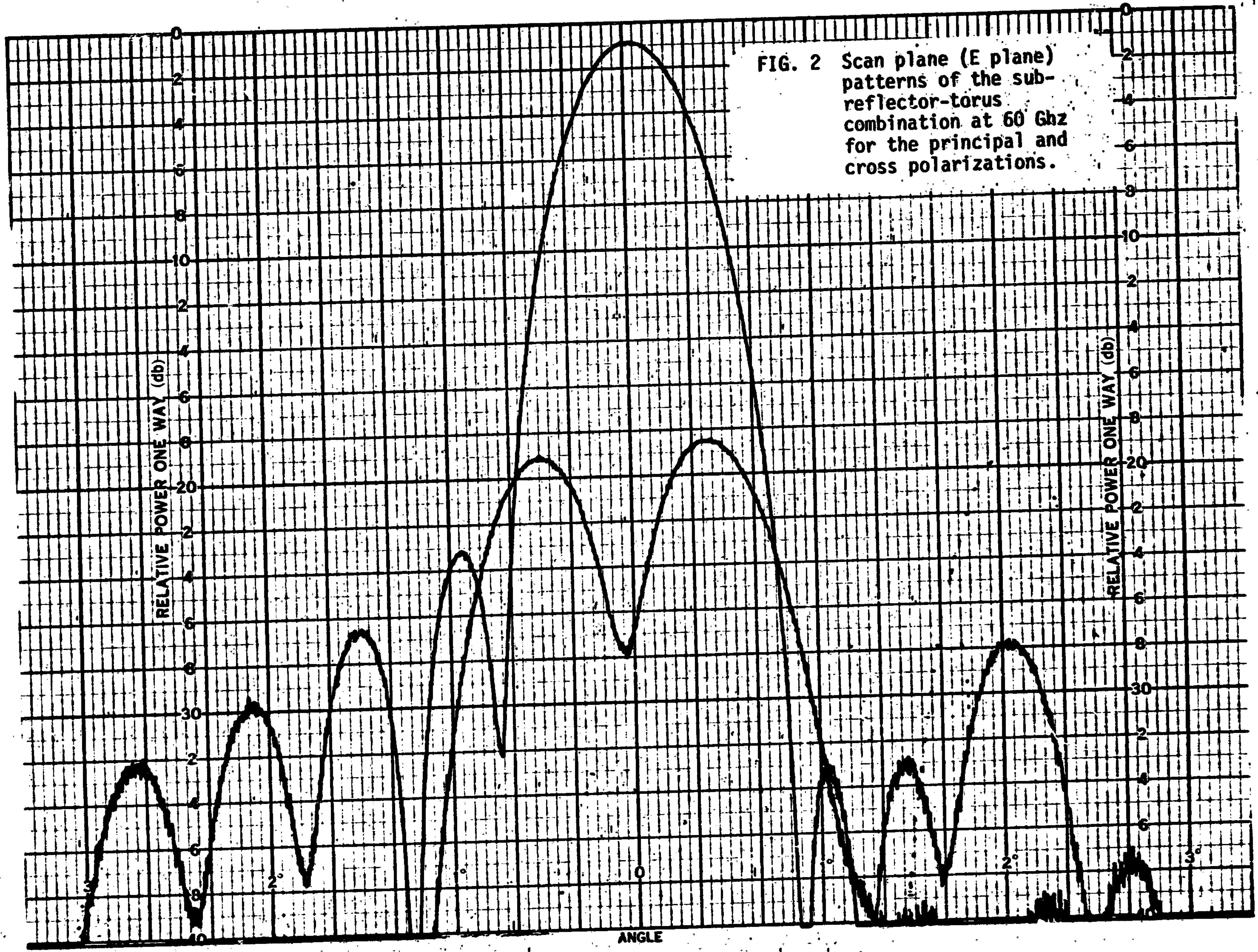

FIG. 2 Scan plane (E plane) patterns of the sub-reflector-torus combination at 60 Ghz for the principal and cross polarizations.

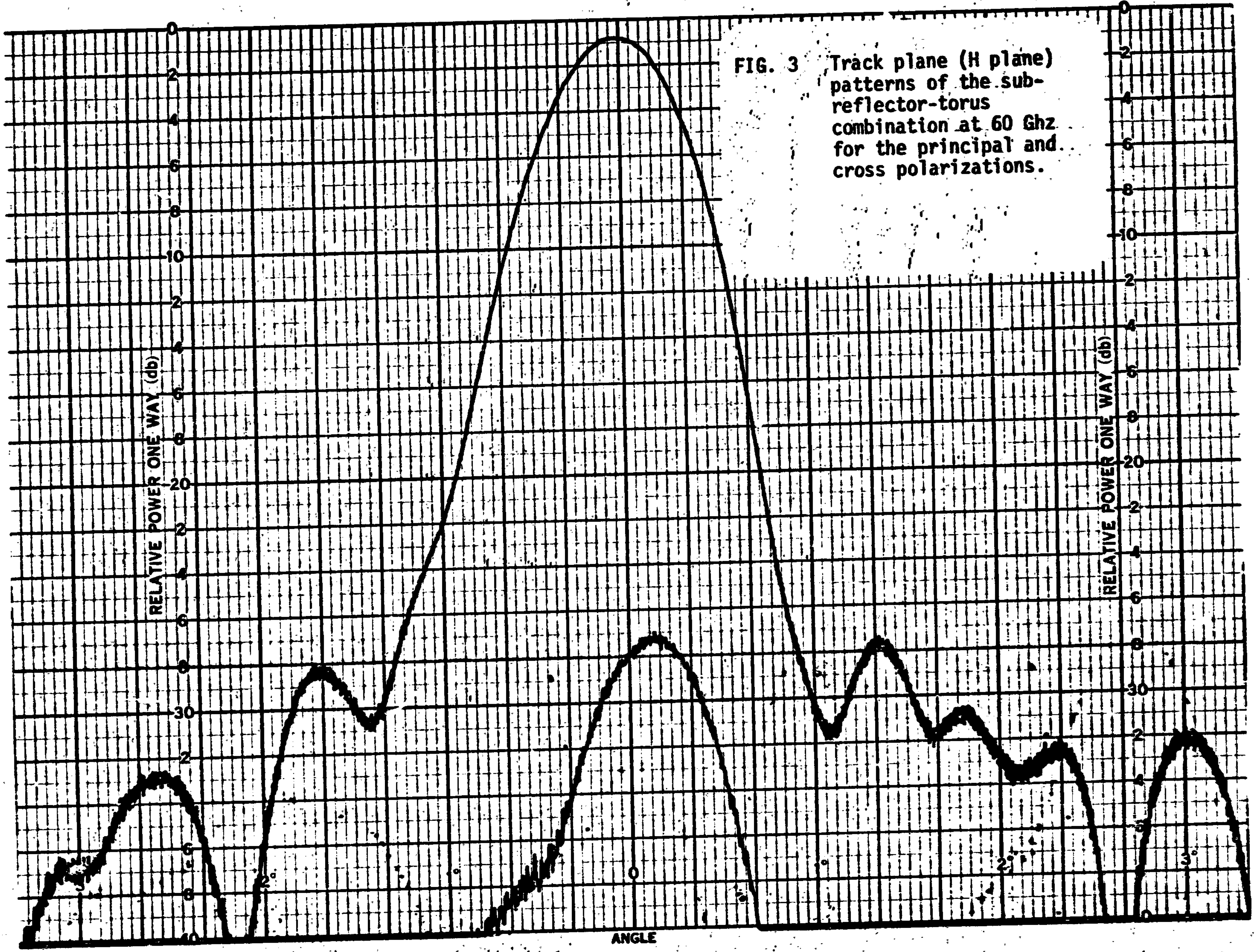

FIG. 3 Track plane (H plane) patterns of the sub-reflector-torus combination at 60 Ghz for the principal and cross polarizations.

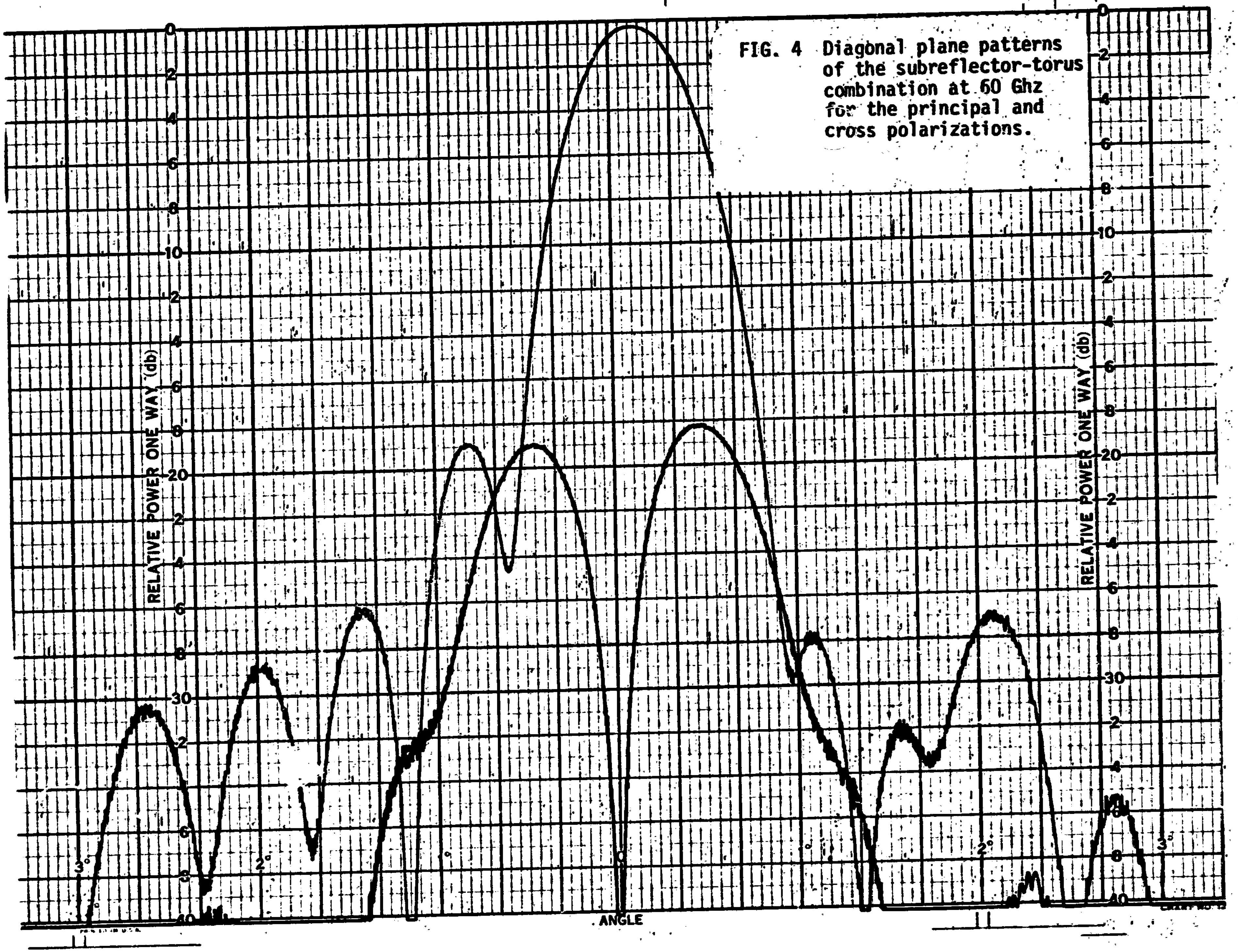

FIG. 4 Diagonal plane patterns of the subreflector-torus combination at 60 Ghz for the principal and cross polarizations.

fact that the geometrical optics analysis assumed a hypothetical Gaussian feed pattern with polarization characteristics similar to that of an elementary current element. The one-third scale model, however utilized a horn feed radiator which has similar properties, but could be sufficiently different to explain the anomaly.

2.2 Ghz Model Measurements

It is of some interest to determine if the subreflector feed technique would work at the longer wavelengths. Limited measurements of the model at 30 Ghz were made to provide some insight into this question since at this frequency the subreflector [illegible] is only 10 wavelengths. E- and H-plane antenna patterns were measured at 30 Ghz and these patterns are presented in Figs. 5 and 6. The patterns were cut with a 30 db dynamic range to show the decaying sidelobe structure. It is clear from these patterns that the model antenna performance at 30 Ghz does not differ appreciably from the performance at 60 Ghz, verifying that the subreflector feed is useable in the full size antenna at frequencies down to at least 10 Ghz.

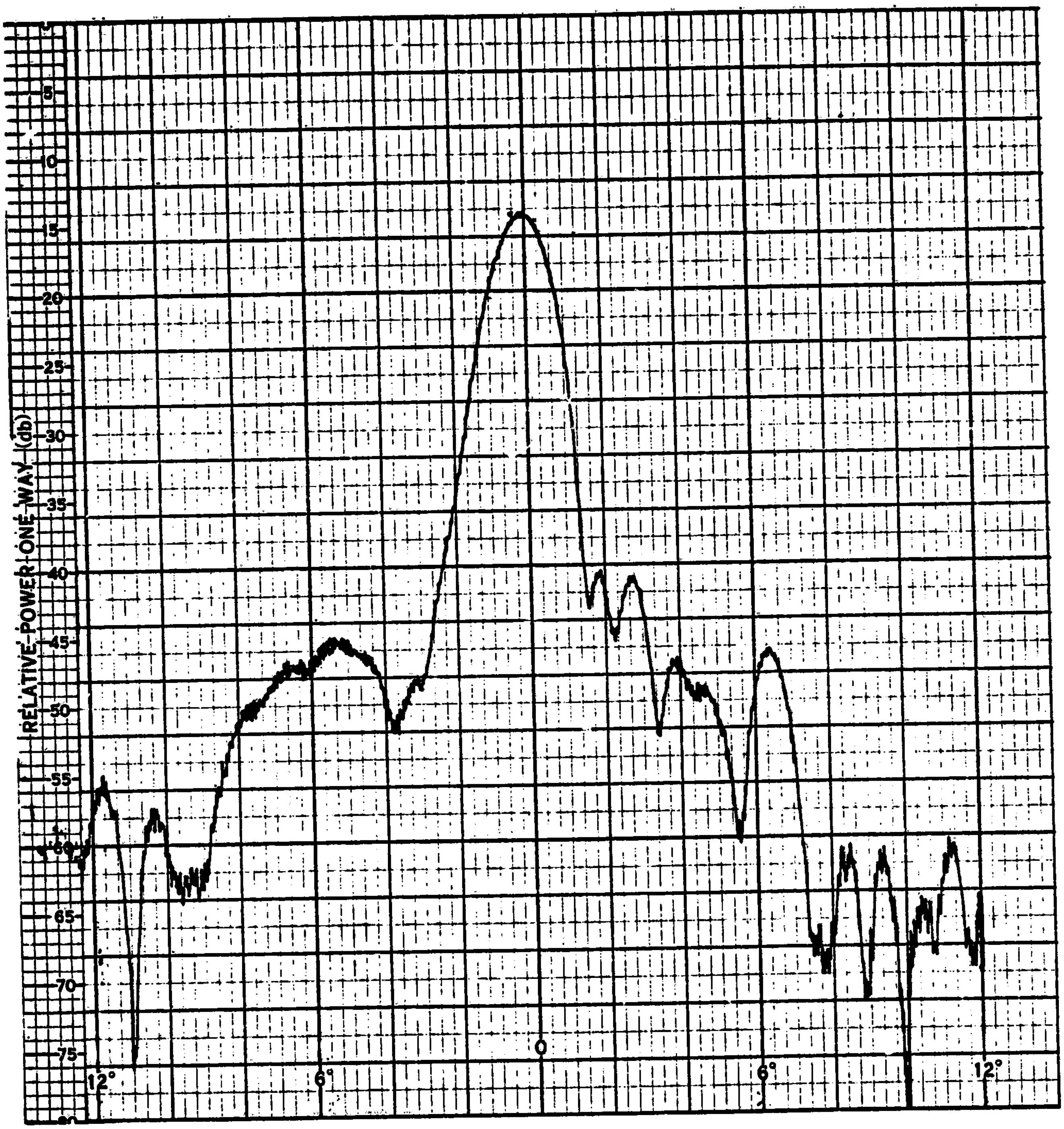

FIG. 5 Track plane (H-plane) pattern of the subreflector-torus combination at 30 Ghz.

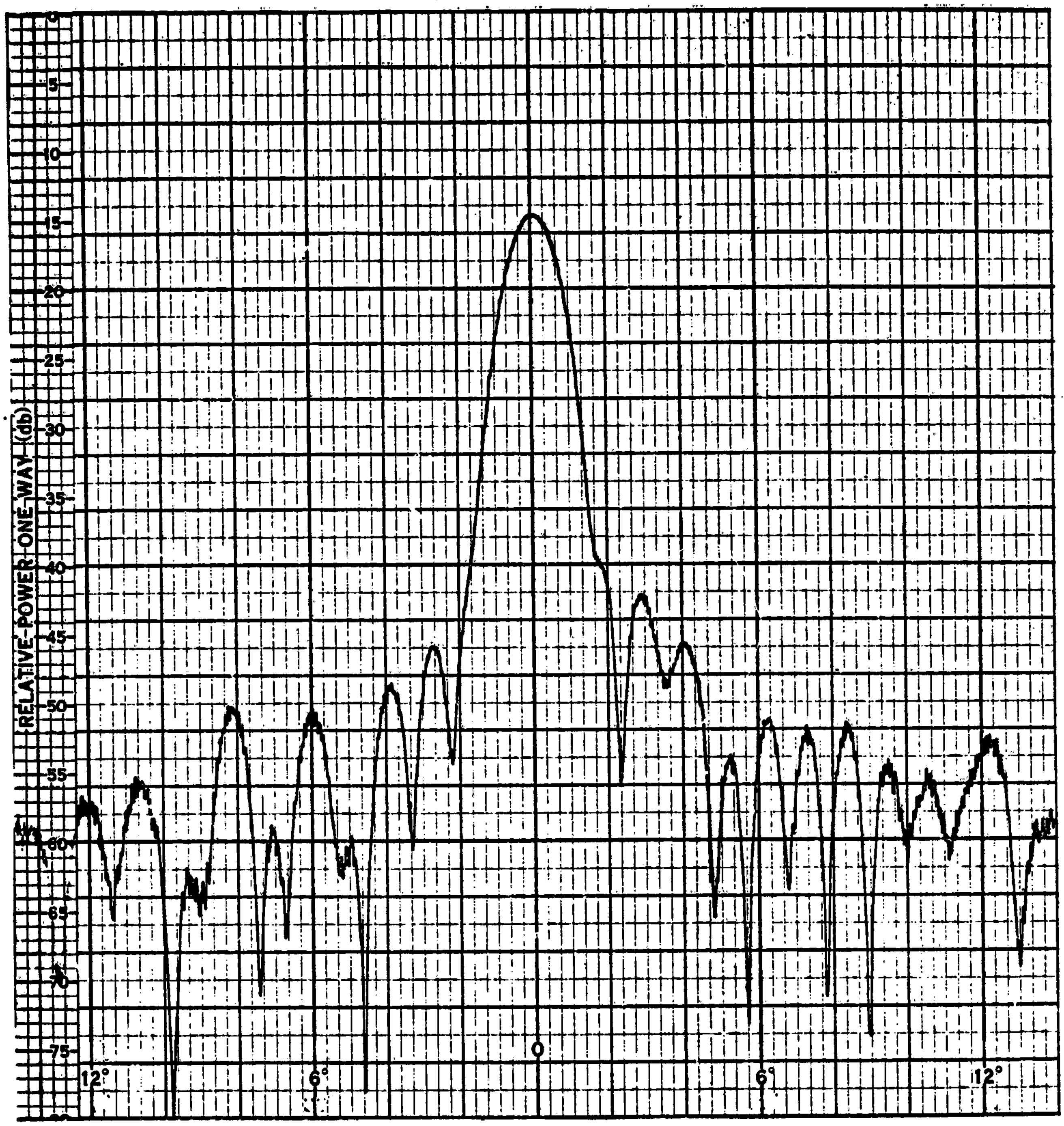

FIG. 6 Scan plane (E-plane) pattern of the subreflector-torus combination at 30 Ghz.

3.0 MODEL ANTENNA DESIGN AND FABRICATION

3.1 Antenna Fabrication Considerations

The primary consideration governing the fabrication of the antenna is that of surface tolerance. Previous studies have indicated that an rms surface tolerance of $\lambda/40$ will render the effects of surface inaccuracies on the antenna beam efficiency negligible. This criteria would then require an rms tolerance of about 0.005" for operation at 60 Ghz. In order to insure that this level would be achieved and in order to make the model antenna useful for other higher frequency applications presently being planned, it was decided that the antenna would be fabricated with the objective of having a peak deviation no greater than 0.005". Such accuracies are well within the scope of standard machining practice.

For the antenna meaurements contemplated for the one-third scale model weight and temperature stability were secondary considerations. It was therefore decided to machine the parabolic main reflector contour directly into an aluminum shell which could be done inexpensively and with extreme precision on a vertical tracer lathe. Preliminary calculations showed that such a shell 0.25" thick would have a weight of 80 lbs. which would be quite reasonable for range work, even with the additional weight of the back-up structure and mounting fixture.

Since the torus would be about 50" in diameter and 25" high some consideration had to be given to problems associated with the fabrication process. The first problem involved the determination of how to fabricate the raw shell and back-up structure into which the contour would be traced. The torus is only one-half of a closed circular shell and distortions due to stresses in machining could seriously effect the circularity of the contour. Attempts to stretch form or bump material into the form of the raw shell would inherently give rise to built-in stresses. Subsequent stress relief operations would be only partially effective and would require a large raw shell wall thickness to insure final clean up thereby substantially increasing the material and machining costs. It was therefore decided that some casting process should be used to generate the raw shell.

The reflector surface is too large to economically cast in one piece and it was therefore decided to form the shell from a series of identical gore sections. This method had the advantage that each gore section could be cast individually along with a gusset and base which would form the reflector back-up structure. This would eliminate the need of welding on the back-up structure thereby introducing stresses into the shell. In addition, since each gore section was of a reasonably small size they could be sand-cast with a fair precision so that the raw shell wall thickness could be minimized.

Investigations were made as to the possibility of welding a seam between each gore section so as to generate one continuous shell surface. It was determined that large distortions of the gore composite would occur due to the welding even to the point that the final weldment would not clean up under machining. This factor and the fact of the stresses, which would be introduced by the welding suggested that the continuous reflector concept be abandoned.

It was decided that the gore sections would be individually machined and assembled side-by-side, held accurately in place by bolting to a base plate on the bottom and an alignment ring on the top. The sides of the gores would be machined with such an accuracy that the cracks between the sections would be less than a few mills and therefore no consequence. The final assembly of the picewise continuous reflector would allow for an accurate adjustment of the gore panel positions into a true figure ot revolution. Finally, only an initial heat treat process would be required to bring the raw castings to a T-6 condition for machining. No stress relief would be required during machining due to the small size of the individual gore sections.

3.2 Gore Pattern and Castings

Fig. 7 shows a drawing of the aluminum pattern from which the gore panels were cast. Each gore section was chosen to be a 30° sector of the parabolic torus. The pattern was constructed by first making a rough male template by bandsawing and filing a 0.09" thick aluminum sheet to a layout line. The template was then mounted on an axle and used to sweep a plaster forming female mold of the curved back surface of the gore. The mold was then covered with release and the template withdrawn 0.5" from the female mold surface by a repositioning of the axle. Plaster was then added to the mold and swept with the template from its new position. After hardening the 0.5" thick plaster equivalent of the required curved gore surface was removed from the mold and reproduced in alumonum by means of sand cast process. The aluminum gore surface was then captured at the top and bottom by the respective lip and base sections into which were machined circular recesses of such

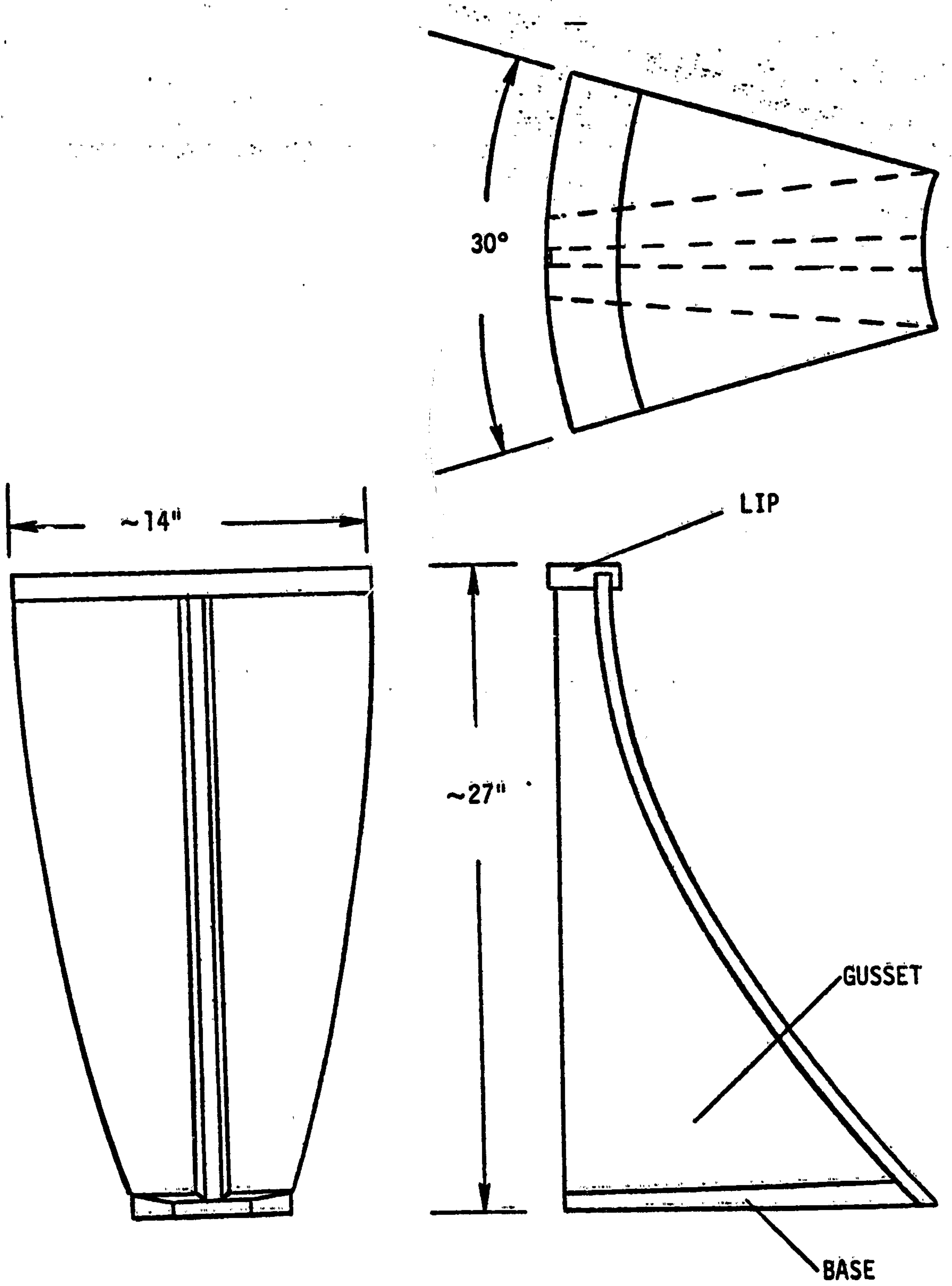

FIG. 7 The gore pattern.

diameters to accurately align the surface. The back gusset was then added and bolted together and the cracks radiused with modeling compound to facilitate sand casting.

The gores were cast from 356 aluminum and heat treated to a T-6 condition. After casting the shrinkage of the casting dimensions from those of the pattern was measured and found to be approximately 1.3%. It was then determined that a radius of the base of the torus of R_o = 25.624" and a torus height of $R_0/2$ = 12.812 would be the best choice of dimensions for producing a final reflector thickness of 0.25" from the castings.

3.3 Template

The template which was used to trace the parabolic profile of the gore sections was machined from 3/16" aluminum plate. The parabolic contour was approximated by ten circular arcs and machined on a continuous path numerically controlled milling machine with a 0.500" diameter end mill. The maximum deviation of the circular arc approximation from the true parabolic curve was computed and found to be 0.00023". The linear separation of the start and end points of the template curve was inspected after the template was machined and found to be true within at least 0.001" which was the lower limit of the inspection equipment used for the measurement.

3.4 Gore Machining and Assembly

Seven 30° gore sector castings were used to form the reflector surface. Two of the sections were split forming two 15° sectors with their respective gussets. These two split sections were used at the ends of the 180° torus to provide maximum strength. The gore castings were first faced off at the top and bottom, drilled and then clamped between two flat fixtures where their locations were accurately determined by means of dowel pins. The edges of the castings were then machined so that the castings could be positioned exactly side by side with a crack no more than a few thousands of an inch wide. Lightening holes were then machined into the gussets and the gores were then screwed down to a 48" square half-inch thick tooling plate. The gores were equally spaced in a circle on the plate so that the resulting geometry was balanced for rotation.

The parabolic contour was then traced into the gore sections on a 48" diameter vertical tracer lathe. Care was taken to achieve a good finish machining with a finish cut of less than .012". After finish machining the large and small diameters at the top and bottom of the torus were inspected and found to be within .001" of their design values.

The machined gore sections were then removed from the tooling plate and mounted on a 0.5" thick aluminum base by means of screws. The lips at the top of the gores were captured in a circular groove machined into a 0.25" x 2.5" ring with a numerically controlled machine thus insuring the circularity of the large diameter at the base of the torus. The circularity of small diameter at the top of the torus was generated by properly aligning the gores as they were screwed to the base plate. This was done by sweeping an indicator pivoted at the torus axis along the edges of the gores at the smaller diameter. After alignment, it was determined that the upper and lower diameters of the reflector were circular within 0.002".

3.5 Subreflector Machining

The fabrication of the subreflector presented the most challenging fabrication problem. The subreflector shape is a totally transcendental three-dimensional curve approximately 8" wide and 4" high. The mathematical technique available to generate the surface coordinates is parametric in nature inasmuch as the subreflector coordinates are not generated directly. For a given point specified in the planar aperture in front of the torus, a numerical computation generates the coordinates of the point on the subreflector through which the ray from the feed reflects to the torus and then out to the specified point.

The machining problem was solved by means of a direct approach. The planar aperture was divided up into 1700 points which were distributed in such a fashion that the resulting 1700 subreflector coordinates generated by the computer were sufficiently closely spaced that a 2" diameter ball mill cutter would generate a faceted approximation to the true surface when moving from point-to-point in straight lines. The maximum deviation from the true surface was estimated to be in the order of .00125". The computer was programmed to directly punch and output a 300 ft. long tape which could command a Bridgeport Series 2 numerically controlled milling machine to execute the required 1700 cutter moves. Human transcribing error was thus completely eliminated. The FORTRAN program used to make the tape is included in Appendix A of this report.

The reflector was hogged out of a cylindrical aluminum blank which was rough machined on a lathe. Several passes were made with a finish machine cut of approximately .010". No inspection of the final surface was possible but from previous experience with the machine used, cutter positioning errors were believ to be in the order of no more than .0002".

3.6 Feed Horns

Horizontally polarized feed horns were constructed by flaring up from a waveguide flange in both the E- and H-planes. The horns were designed to produce 3 db beamwidths of 30° in the H-plane and 60° in the E-plane. To generate this performance an E-plane aperture dimension of .887λ and an H-plane dimension of 2.23λ were selected. The resulting aperture dimensions were .174" x .439" for the 60 Ghz horn and .348" x .878" for the 30 Ghz horn. The 60 Ghz horn was 1.875" in length and designed with a WR 15 waveguide flange. The 30 Ghz horn was 3.000" in length with a WR 28 waveguide flange. Antenna patterns of the 60 Ghz horn were measured and are shown in Figs. 8, 9 and 10 for the principal planes and diagonal plane cut at a frequency of 59.35 Ghz. Cross polarization patterns are also shown. As seen in the figures the measured 3 db beamwidths are 30° for the H-plane, 54° for the E-plane and 40° for the diagonal plane. The observed cross polarization levels are in excess of -22 db and probably due to range errors.

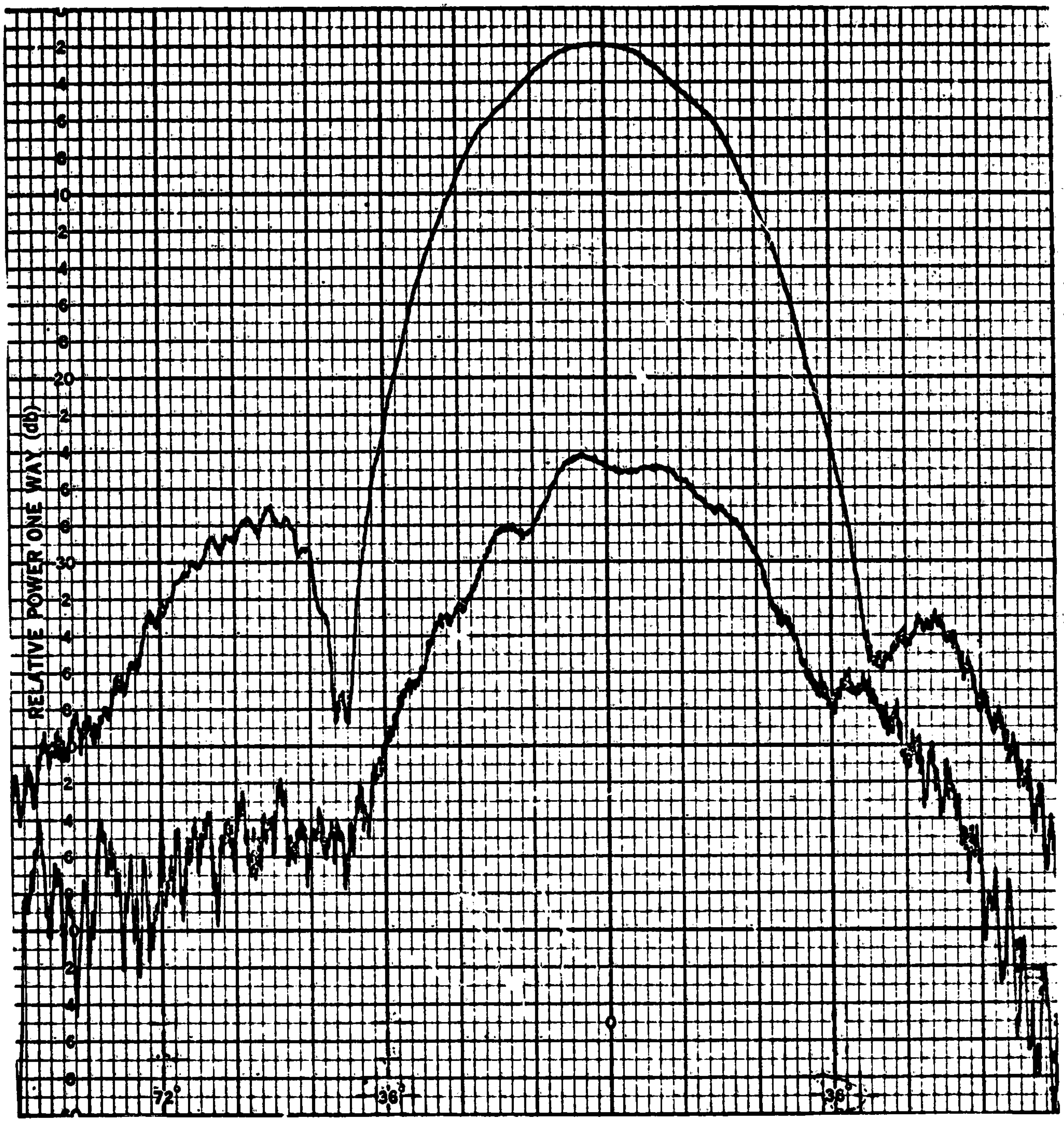

FIG. 8 H-plane feed patterns at 59.35 Ghz for the principal and cross polarizations.

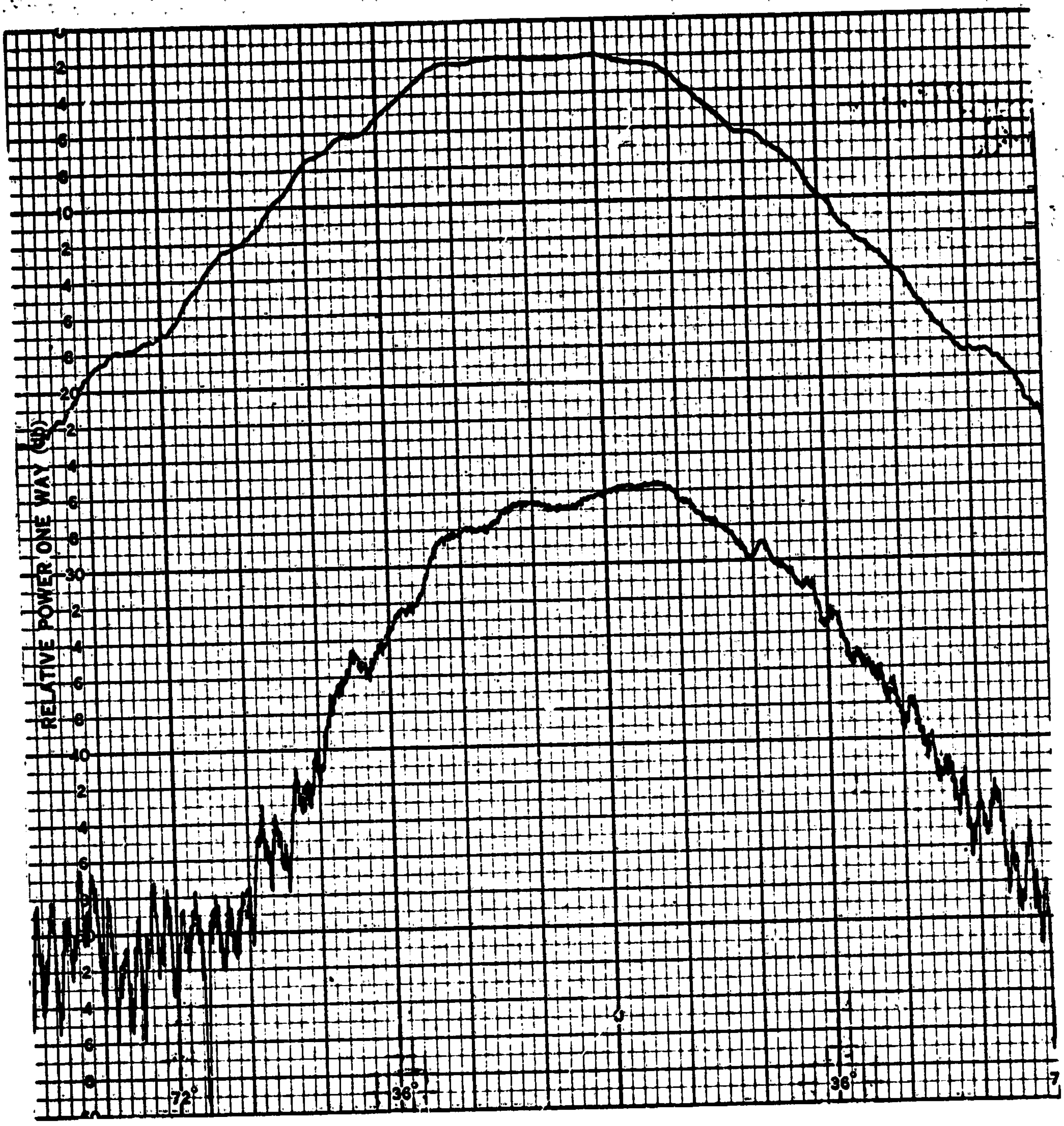

FIG. 9 E-plane feed patterns at 59.35 Ghz for the principal and cross polarizations.

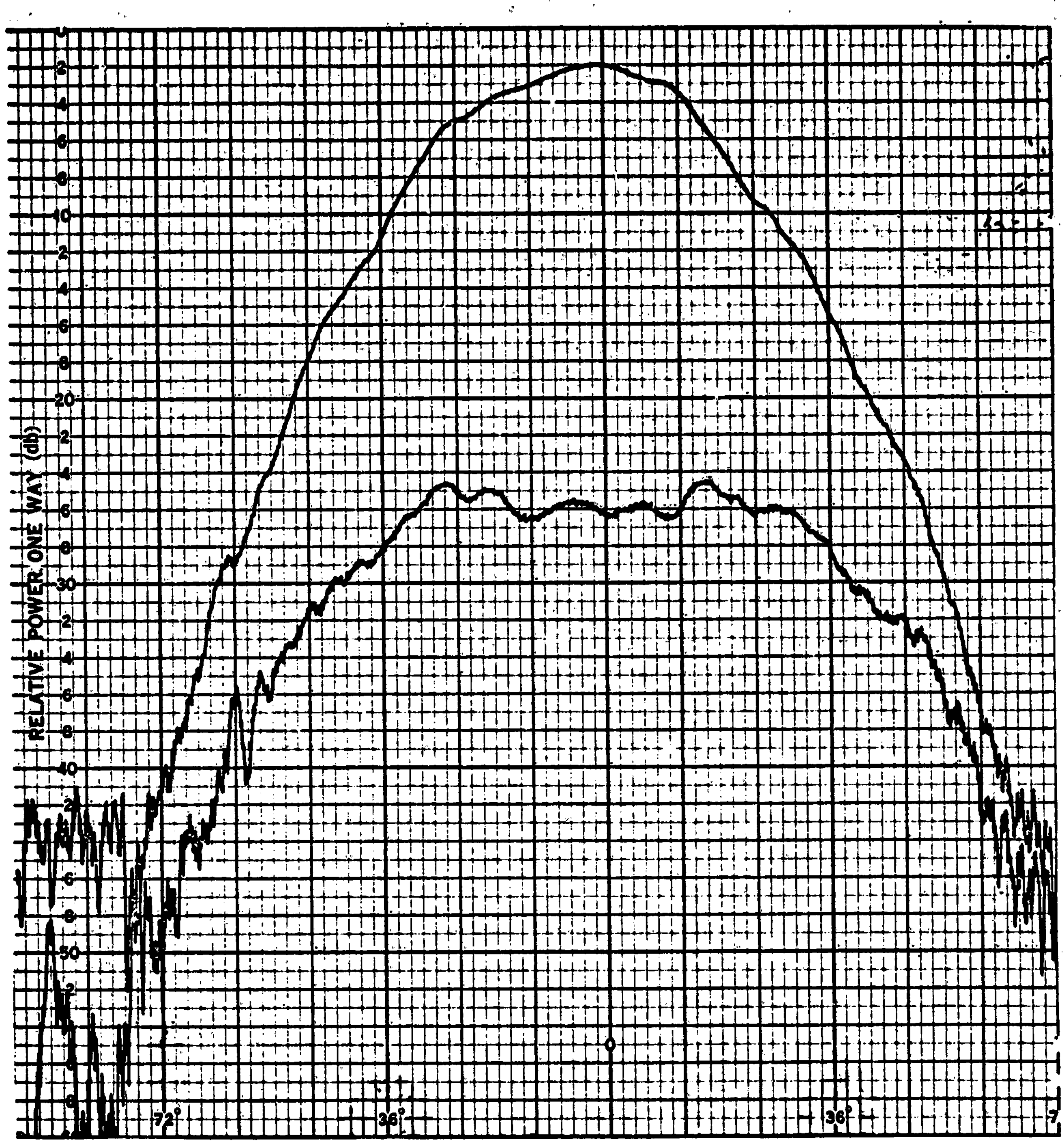

FIG. 10 Diagonal plane feed patterns at 59.35 Ghz for the principal and cross polarizations.

4.0 CONCLUSIONS AND RECOMMENDATIONS

The satisfactory performance of the 4m SIMS parabolic torus reflector with a Gregorian subreflector feed has been verified both experimentally and theoretically at frequencies above 10 Ghz.

It is recommended that any further experimental studies should include an investigation of the antenna performance near the edges of the range of scan to observe the end effects of the torus reflector. Also, it is recommended that a study be performed to examine the effects of feed displacement with the objective of determining the feasibility of clustering independent feed horns side-by-side in the subreflector.

5.0 NEW TECHNOLOGY

No reportable items of new technology have been identified in the work described in this report.

6.0 REFERENCES

1. Gustincic, J.J.; "Design of an Offset Fed Scanning Antenna for the Shuttle Imaging Microwave System," JPL Contract No. 954145, Report No. TR 070, 14 April 1975.

7.0 APPENDIX A

SUBREFLECTOR CUTTER POSITION PROGRAM

```
      NAMELIST/DATA/H,F,S,A,AZBW,ELBW
      NAMELIST/DATA2/SUMX
      REAL NX,NY,NZ,MX,MY,MZ,K
      REAL  XLIST(42,42)/1764*0.0/,YLIST(42,42)/1764*0.0/,ZLIST(42,42)
     * /1764*0.0/
      REAL SUMX(41)/41*0.0/
      READ(5,DATA)
      I=1
      J=1
      RAD=1.
      Z=0
1     X=0
      HOLDX=0.
      IF (Z.GT..8)  GO TO 5
2     Y= SQRT(ABS(  (1.-Z**2/2.)**2 - X**2) )
      NZ = SQRT(1.+Z**2)
      NY = SQRT(X**2 + Y**2)
      NX = -X/(NZ*NY)
      NY = -Y/(NZ*NY)
      NZ = -Z/NZ
      MX = -2.*NY*NX
      MY = 1. -2.*NY*NY
      MZ = -2.*NY*NZ
      K = 2. -S + SQRT(H**2 + (F-S)**2 )
      C= .5*((K-Y)**2-X**2-(Y-F)**2-(Z+H)**2)/
     * (K-Y+MX*X+MY*(Y-F)+MZ*(Z+H) )
      XX = -X - C*MX
      YY = F - Y - C*MY
      ZZ = Z + H + C*MZ
      ARX = K-C-Y
      ARY = -YY/ARX
      ARZ = ZZ/ARX
      ARX = -XX/ARX
      UX = MX + ARX
      UY = MY + ARY
      UZ = MZ + ARZ
      UM= -SQRT(UX**2+UY**2+UZ**2)
      XXP= 25.624*XX- UX*RAD/UM
      YYP= 25.624*YY- UY*RAD/UM
      ZZP=25.624*ZZ+ UZ*RAD/UM
      IF (J.NE.1)  GO TO 9
11    XLIST(I,J)= XXP
      IF ((1000.*XLIST(I,J)-AINT(1000.*XLIST(I,J))).GE..5)   XLIST(I,J)
     * =XLIST(I,J)+.001
      XLIST(I,J)= AINT(1000.*XLIST(I,J))/1000.
```

ORIGINAL PAGE IS
OF POOR QUALITY

```
      YLIST(I,J)= YYP
      ZLIST(I,J)= ZZP
      J= J+1
      GO TO 3
9     IF (XXP- XLIST(I,J-1)-.15)  10,11,12
10    HOLDX= XXP
      HOLDY= YYP
      HOLDZ= ZZP
      GO TO 3
12    IF (HOLDX.NE.XLIST(I,J-1))  GO TO 13
      HOLDX= XXP
      HOLDY= YYP
      HOLDZ= ZZP
13    XLIST(I,J)= HOLDX
      IF ((1000.*XLIST(I,J)-AINT(1000.*XLIST(I,J))).GE..5)   XLIST(I,J)
     * =XLIST(I,J)+.001
      XLIST(I,J)= AINT(1000.*XLIST(I,J))/1000.
      YLIST(I,J)= HOLDY
      ZLIST(I,J)= HOLDZ
      HOLDX= XXP
      HOLDY= YYP
      HOLDZ= ZZP
      J= J+1
3     X=X+.01
50    IF(Z-.1)    51,51,52
51    IF (X-.3)       2,2,4
52    IF(Z-.2)    53,53,54
53    IF (X-Z-.2)    2,2,4
54    IF(Z-.4)    55,55,56
55    IF (X-.4)       2,2,4
56    IF(Z-.6)    57,57,58
57    IF (X-.6+(Z/2.))   2,2,4
58    IF(Z-.8)    59,60,5
59    IF (X+Z-.9)     2,2,4
60    IF (X-.1)       2,2,5
4     Z= Z+.02
      IF (XLIST(I,J-1).EQ.XXP)  GO TO 6
      XLIST(I,J)= HOLDX
      IF ((1000.*XLIST(I,J)-AINT(1000.*XLIST(I,J))).GE..5)   XLIST(I,J)
     * =XLIST(I,J)+.001
      XLIST(I,J)= AINT(1000.*XLIST(I,J))/1000.
      YLIST(I,J)= HOLDY
      ZLIST(I,J)= HOLDZ
6     I= I+1
      J= 1
      GO TO 1
5     CONTINUE
```

ORIGINAL PAGE IS
OF POOR QUALITY

```
20    FORMAT (I2,3(-,-,F6.3),-$-)
      I= 1
14    J= 42
15    IF (XLIST(I,J).NE.0.)  GO TO 16
      J= J-1
      GO TO 15
16    XMOVE= -XLIST(I,J)
      YMOVE=  YLIST(I,J)
      ZMOVE=  ZLIST(I,J)
      PUNCH  20,I,XMOVE,YMOVE,ZMOVE
      SUMX(I)= SUMX(I)+ XMOVE
17    XMOVE= XLIST(I,J)- XLIST(I,J-1)
      YMOVE= YLIST(I,J-1)- YLIST(I,J)
      ZMOVE= ZLIST(I,J-1)- ZLIST(I,J)
      PUNCH  20,I,XMOVE,YMOVE,ZMOVE
      SUMX(I)= SUMX(I)+ XMOVE
      J= J-1
      IF (J.GT.1)  GO TO 17
18    XMOVE= XLIST(I,J+1)- XLIST(I,J)
      YMOVE= YLIST(I,J+1)- YLIST(I,J)
      ZMOVE= ZLIST(I,J+1)- ZLIST(I,J)
      PUNCH  20,I,XMOVE,YMOVE,ZMOVE
      SUMX(I)= SUMX(I)+ XMOVE
      J= J+1
      IF (XLIST(I,J+1).NE.0.)  GO TO 18
      XMOVE= -XLIST(I,J)
      YMOVE= -YLIST(I,J)
      ZMOVE= -ZLIST(I,J)
      PUNCH  20,I,XMOVE,YMOVE,ZMOVE
      SUMX(I)= SUMX(I)+ XMOVE
      I= I+1
      IF (I.LE.41)  GO TO 14
      WRITE(6,DATA2)
      STOP
      END
 -XQT
  9DATA H=.0813,F=.5625,S=.4000,A=1.,A2BW=60.,ELBW=31. 9END
```

ORIGINAL PAGE IS
OF POOR QUALITY